Mol Cell Biochem (2015) 403:287–299
DOI 10.1007/s11010-015-2358-6

Fibroblast growth factor (FGF21) protects mouse liver against D-galactose-induced oxidative stress and apoptosis via activating Nrf2 and PI3K/Akt pathways

Yinhang Yu · Fuliang Bai · Yaonan Liu · Yongbi Yang · Qingyan Yuan · Dehua Zou · Susu Qu · Guiyou Tian · Liying Song · Tong Zhang · Siming Li · YunYe Liu · Wenfei Wang · Guiping Ren · Deshan Li

Received: 8 October 2014 / Accepted: 14 February 2015 / Published online: 21 February 2015

Abstract FGF21 is recently discovered with pleiotropic effects on glucose and lipid metabolism. However, the potential protective effect of FGF21 against D-gal-induced injury in the liver has not been demonstrated. The aim of this study is to investigate the pathophysiological role of FGF21 on hepatic oxidative injury and apoptosis in mice induced by D-gal. The 3-month-old Kunming mice were subcutaneously injected with D-gal (180 mg kg^{-1} d^{-1}) for 8 weeks and administered simultaneously with FGF21 (5 or 1 mg kg^{-1} d^{-1}). Our results showed that the administration of FGF21 significantly alleviated histological lesion including structure damage, degeneration, and necrosis of hepatocytes induced by D-gal, and attenuated the elevation of liver injury markers, serum AST, and ALP in a dose-dependent manner. FGF21 treatment also suppressed D-gal-induced profound elevation of ROS production and oxidative stress, as evidenced by an increase of the MDA level and depletion of the intracellular GSH level in the liver, and restored the activities of antioxidant enzymes SOD, CAT, GSH-Px, and T-AOC. Moreover, FGF21 treatment increased the nuclear abundance of Nrf2 and subsequent up regulation of several antioxidant genes. Furthermore, a TUNEL assay showed that D-gal-induced apoptosis in the mouse liver was significantly inhibited by FGF21. The expression of caspase-3 was markedly inhibited by the treatment of FGF21 in the liver of D-gal-treated mice. The levels of PI3K and PBK/Akt were also largely enhanced, which in turn inactivated pro-apoptotic signaling events, restoring the balance between pro- and anti-apoptotic Bcl-2 and Bax proteins in the liver of D-gal-treated mice. In conclusion, these results suggest that FGF21 protects the mouse liver against D-gal-induced hepatocyte oxidative stress via enhancing Nrf2-mediated antioxidant capacity and apoptosis via activating PI3K/Akt pathway.

Keywords FGF21 · D-Gal · Nrf2-mediated antioxidant capacity · PI3K/AKT · Apoptosis

Yinhang Yu and Fuliang Bai have contributed equally to this study and are co-first authors.

Electronic supplementary material The online version of this article (doi:10.1007/s11010-015-2358-6) contains supplementary material, which is available to authorized users.

Y. Yu · F. Bai · Y. Liu · Y. Yang · Q. Yuan · G. Tian · L. Song · T. Zhang · Y. Liu · W. Wang · G. Ren (✉) · D. Li (✉)
Bio-pharmaceutical Lab, Life Science College, Northeast Agricultural University, Harbin 150030, China
e-mail: renguiping@126.com

D. Li
e-mail: deshanli@163.com

D. Zou
Heilongjiang Bayi Agricultural University, Daqing 163319, China

S. Qu
Institute of Psychology, Chinese Academy of Sciences, Beijing 100101, China

S. Li
Harbin University of Commerce, Harbin 150028, China

W. Wang · G. Ren · D. Li
Key Laboratory of Agricultural Biological Function Gene, Northeast Agricultural University, Harbin 150030, China

Abbreviations

FGF21	Fibroblast growth factor 21
D-Gal	D-Galactose
AST	Aspartate aminotransferase
ALP	Alkaline phosphatase
ROS	Reactive oxygen species
MDA	Malondialdehyde
GSH	Glutathione
SOD	Superoxide dismutase
CAT	Catalase
GSH-Px	Glutathione peroxidase
T-AOC	Total antioxidation capability
Nrf2	Nuclear factor erythroid 2-related factor 2
TUNEL	Terminal deoxynucleotidyl transferase (TdT)-mediated dUTP nick end labeling
PI3K	Phosphoinositide-3-kinase
PBK/Akt	Protein kinase B

Introduction

Increasing evidence has demonstrated that oxidants play important roles in aging [1]. D-Galactose (D-gal) is present in many food products and can also be synthesized by the body, where it forms part of glycolipids and glycoproteins. It is normally metabolized by D-galactokinase and galactose-1-phosphate uridyltransferase, while at levels greater than normal, D-gal can promote the generation of reactive oxygen species (ROS) and the formation of advanced glycation end-products (AGE) within cells, which in turn result in oxidative stress and cellular damage in animal tissues. Chronic administration of D-gal-induced changes resembled natural aging in rodents [2, 3]. More researches demonstrated that D-gal treatment caused oxidative stress and mitochondrial dysfunction in the livers of mice and rats [4, 5]. These oxidative stress-induced damages disrupt cellular function and membrane integrity, thereby leading to apoptosis [6, 7].

In the antioxidant defense system, nuclear factor erythroid 2-related factor 2 (Nrf2) is one of the most important transcription factors in regulating multiple antioxidants, which binds to the antioxidant response elements (AREs) and has been demonstrated to be a critical transcription factor in the promoter region of a number of genes, encoding for antioxidative and phase 2 enzymes, such as hemeoxygenase 1 (HO-1) and glutamate cysteine ligase (GCL), and plays a critical role in the regulation of the cellular GSH homeostasis [8, 9]. Apoptosis is a form of programmed cell death and plays an important role in a variety of physiological and pathological processes [10]. The phosphoinositide-3-kinase (PI3K)-Akt signaling pathway plays a crucial role in cell growth and cell survival [11], which can be activated by many types of cellular stimuli or toxic insults, and can also mediate some of its survival signals through the Bcl-2 family [12].

Fibroblast growth factor 21 (FGF21), as a member of the FGF family secreted predominantly by the liver, pancreas, and adipose tissues is identified as a critical regulator of long-term energy balance, glucose, and lipid homeostasis [13–15]. Recently, there is increasing evidence that FGF21 has the function in suppression of inflammation, oxidative stress, and the fibrotic effect [16–18]. In addition, FGF21 can regulate ketogenesis, gluconeogenesis, and growth hormone resistance in the liver, and protect against acetaminophen-induced liver failure in mice [19–22]. As previously described, many researches indicated that FGF21 exerts a potentially beneficial protective effect on organ injury. However, little work has been done to explore the underlying mechanism of hepatoprotective effects of FGF21 on D-gal-induced liver injury.

It is well known that oxidative stress leads to apoptosis and apoptosis contributes to liver injury in many acute and chronic liver injuries [7, 23]. Therefore, the aim of this study is to explore whether FGF21 protected mouse liver from D-gal-induced injury by attenuating oxidative stress and suppressing apoptosis pathway.

Materials and methods

Animals and treatments

Ethics statement

All experiments were carried out in strict accordance with the recommendations of the Guide for the Care and Use of Laboratory Animals of the National Institutes of Health and were approved by Harbin Veterinary Research Institute Animal Care and Use Committee.

Eight-week-old male Kunming mice were purchased from Wei tong li hua Animal Center (Beijing, China). The mice were maintained under constant conditions (23 ± 1 °C and 60 % humidity) and had free access to rodent food and tap water. Eight mice were housed per cage on a 12-h light/dark schedule (lights on 08:30–20:30). At 12 weeks of age (37.1 ± 0.6 g), mice were randomly divided into four groups ($n = 8$ per group), groups 2-4 received daily subcutaneous injection of D-gal (Sigma-Aldrich, MO, USA) at dose of 180 mg kg^{-1} d^{-1} for 8 weeks and group 1 as normal control with injection of saline (0.9 %) only. Meanwhile, group 3 and 4 D-gal-treated mice received simultaneously FGF21 of 5 or 1 mg kg^{-1} d^{-1}. Then, mice were sacrificed and the livers were immediately collected, respectively for experiments or stored at −70 °C for later use.

Histological evaluations

For pathological studies, the liver tissues were fixed in a fresh solution of 4 % paraformaldehyde (pH 7.4) for 24 h, then postfixed in 70 % ethanol for at least 12 h. After dehydration, the liver was embedded in paraffin blocks. 2-μm-thick sections obtained from each paraffin block were stained with hematoxylin and eosin (H & E) for histopathological evaluation under digital light microscope Leica Camera (Germany).

Liver function test

Serum was obtained by centrifugation at $1100\times g$ for 10 min and stored at −80 °C until needed. Serum alanine aminotransferase (ALT), aspartate aminotransferase (AST), alkaline phosphatase (ALP), total bilirubin (TBIL) and direct bilirubin (DBIL) levels were measured by immuno enzymatic assays.

Assay of ROS

To measure ROS production, the liver ROS generation was determined in tissue homogenates by using dichlorofluorescein diacetate (DCFH-DA) (Jiancheng Institute of Biotechnology, Nanjing China) as a probe according to the previous literature [31]. Briefly, the homogenate was diluted 1:20 (v/v) with PBS buffer (200 mM NaCl, 3 mM KCl, 10 mM Na_2HPO_3, 2.0 mM KH_2PO_3 pH 7.4). The reaction mixture (200 ul) containing 190 ul of homogenate and 10 μl of 1 mM 2′,7′-dichlorodihydrofluorescein diacetate was incubated for 30 min at 37 °C temperature to allow the 2′,7′-dichlorodihydrofluorescein diacetate to be incorporated into any membrane-bound vesicles and the diacetate group to be cleaved by esterases. The conversion of 2′,7′-dichlorodihydrofluorescein diacetate to the fluorescent product 2′,7′-dichlorofluorescein was measured using a spectrofluorometer (PerkinElmer, America) with excitation at 484 nm and emission at 530 nm. Background fluorescence (190 ul homogenate, 10 ul PBS absence of 2′,7′-dichlorodihydrofluorescein) was corrected by the inclusion of parallel blanks. ROS formation was quantified from a 2′,7′-dichlorofluorescein standard curve, and the data are expressed as pmol 2′,7′-dichlorofluorescein formed/min/mg protein.

Determination of redox status

Assay of MDA level

To determine the activity of MDA, we used a commercial kit (Beyotime Institute of Biotechnology, Suzhou, China) to quantify the generation of malondialdehyde (MDA) according to the manufacturer's protocol. In brief, the liver tissues were incubated in the lysate buffer (150 mM NaCl, 1 % N-40, 0.5 % deoxycholate, 1 % Triton X-100, 50 mM Tris–hydrochloric acid, 2 mM phenylmethylsulfonyl fluoride, and proteinase inhibitor cocktail, pH 7.4). After grinding, lysed cells were centrifuged at $10{,}000\times g$ for 5 min to remove debris. The supernatant was subjected to the measurement of MDA levels. The MDA levels were determined at 532 nm using tetra methoxypropane as standard. The results were expressed as the contents nmol per mg protein.

Assay of GSH level

GSH content was determined using a thiol-specific reagent, dithionitrobenzoic acid (DTNB) according to the manufacturer's protocol (Nanjing Jiancheng Bioengineering Institute), and the adduct was measured spectrophotometrically at 420 nm. GSH content was expressed as umol per mg protein.

Assay of SOD activity

SOD activity was measured using an assay kit (Beyotime Institute of Biotechnology, Suzhou, China) with nitroblue tetrazolium substances according to the manufacturer's introduction. Absorbance was read at 550 nm and the activity of SOD was calculated using the formula: [(control value − blank value) − (sample value − blank value)]/(-control value − blank value) × 2 × (total volume/sample volume)/protein concentration.

Assay of GSH-Px activity

GSH-PX activity assay was based on the method of Paglia and Valentine (1967). *tert*-Butylhydroperoxide was used as a substrate. The assay measures the enzymatic reduction of H_2O_2 by GSH-PX through consumption of reduced glutathione (GSH) that is restored from oxidized glutathione GSSG in a coupled enzymatic reaction by GR. GR reduces GSSG to GSH using NADPH as a reducing agent. The decrease in absorbance at 340 nm due to NADPH consumption was measured in a Molecular Devices M2 plate reader (Molecular Devices, Menlo. Park, CA). GSH-PX activity was computed using the molar extinction coefficient of 6.22 mM^{-1} cm^{-1}. One unit of GSH-PX was defined as the amount of enzyme that catalyzed the oxidation of 1.0 mol of NADPH to NADP + per minute at 25 °C.

Assay of CAT activity

CAT activity was measured using a kit (Jiancheng Institute of Biotechnology, Nanjing China); the result was

determined by measuring the intensity of a yellow complex formed by molybdate and H_2O_2 at 405 nm, after ammonium molybdate was added to terminate the H_2O_2 degradation reaction catalyzed by CAT. An enzyme activity unit was defined as degradation of 1 umol H_2O_2 per sec per mg tissue protein, and the enzymatic activity was expressed as U/mg protein.

Assay of T-AOC activity

T-AOC activity was measured using a kit (Jiancheng Institute of Biotechnology, Nanjing China). The antioxidants of liver tissues can make Fe^{3+} to Fe^{2+}, and the solid substances can be formed after Fe^{2+} reacting with phenanthroline substances. The result can be measured spectrophotometrically at 520 nm.

RNA isolation and real-time quantitative PCR

Total RNA from the livers was isolated with Trizol (Invitrogen), and RNA was reverse transcribed into cDNA using the reverse-transcription kit (Promega, USA). The cDNA was used for real-time quantitative PCR (ABI 7500, Applied Biosystems, Carlsbad, CA, USA) with SYBR Green Master Mix and melting curve to detect the following genes: γ-glutamylcysteine ligase catalytic subunit (GCL-c: F: GTT ATG GCT TTG AGT GCT GCA T; R: ATC ACT CCC CAG CGA CAA TC), glutathione peroxidase-1 (Gpx-1: F: CCA GGA GAA TGG CAA GAA TGA; R: TCT CAC CAT TCA CTT CGC ACT T), superoxide dismutase-2 (Sod2: F: TCC CAG ACC TGC CTT ACG ACT AT; R: GGT GGC GTT GAG ATT GTT CA), glucose-6-phosphate dehydrogenase (G6pdh: F: CTG GAA CCG CAT CAT CGT GGA G; R: CCT GAT GAT CCC AAA TTC ATC AAA ATA G), P21: (F: GCA GAT CCA CAG CGA TAT CC; R: CAA CTG CTC ACT GTC CAC GG), Nrf2: (F: GAT CCG CCA GCT ACT CCC AGG TTG; R: AGC ACA CGT TTA TTC ACG GGT), and β-actin: (F: ACA TCT GCT GGA AGG TGG AC; R: GGT ACC ACC ATG TAC CCA GG). The amplified PCR products were quantified by measuring the calculated cycle thresholds (Ct) of samples mRNA and β-actin mRNA. Relative multiples of change in mRNA expression were calculated by $2^{-\Delta\Delta Ct}$. The mean value of normal group target levels became the calibrator (one per sample) and the results are expressed as the n-fold difference relative to normal controls (relative expression levels).

Terminal deoxynucleotidyl transferase-mediated dUTP nick end labeling (TUNEL) assay

Kidney tissue was fixed in 10 % formalin and embedded in paraffin. Fixed liver tissues embedded in paraffin were cut into 4-um thick. After deparaffinization (using xylene and ethanol dilutions) and rehydration, the sections were stained for TUNEL with a DeadEnd™ Colorimetric Apoptosis Detection Kit (Promega, USA) according to the manufacturer's instructions. Briefly, each slide was deparaffinized and rehydrated, and treated with proteinase K (20 ug/mL) for 15 min, and then incubated with the TUNEL reaction mixture containing terminal deoxynucleotidyl transferase (TdT) and digoxigenin-11-dUTP for 1 h. TdT reaction was carried out in a humidified chamber at 37 °C. The endogenous peroxidase was inhibited with 0.3 % hydrogen peroxide for 5 min, and then added Streptavidin HRP for 30 min at room temperature. After that 3,3-diaminobenzidine chromogen was applied. Hematoxylin was used as counterstaining. For the negative control, TdT was omitted from the reaction mixture. TUNEL-positive cells were counted in at least 25 randomly selected fields per group (5 mice per group), and the mean of TUNEL-positive cells from five fields per mouse liver was calculated for further statistical analysis.

Western blotting

Liver tissue was homogenized in a Western and IP lysate buffer containing 0.5 % Triton X-100 and protease-inhibitor cocktail (Beyotime Institute of Biotechnology, Suzhou, China) and the resulting lysate was centrifuged at 12,000 rpm and 4 °C for 5 min. Aliquots of the supernatant were removed for protein analysis by the BCA method. For Nrf2 protein detection, cytoplasmic and nuclear extracts were prepared using the Nuclear and Cytoplasmic Protein Extraction Kit (Beyotime Institute of Biotechnology, Suzhou, China) according to the manufacturer's instructions. The supernatant was incubated at 95 °C for 5 min in SDS sample buffer containing 100 mmol/L DTT, and 20 μg of the sample was then resolved by 12 % SDS-PAGE at 100 V, and then transferred to a nitrocellulose membrane (GE Healthcare). After blocking with 5 % skimmed milk for 1 h, and incubated overnight at 4 °C with the following antibodies: anti-Nrf2, anti-PI3K, anti-phospho-Akt (Ser473), anti-Akt, anti-caspase-3, anti-Bcl-2 and anti-Bax (1:1000 Cell Signaling Technology, Danvers, MA), anti-Laminb1 (1:5000 Affinity Biosciences), and anti-β-actin (1:3000 Signalway USA). Then followed by a horseradish peroxidase-conjugated anti-rabbit or anti-mouse IgG secondary antibody (1:8000) 1 h at room temperature. Blots were visualized using an enhanced chemi-luminescence detection kit (ECL; Thermo Scientific, IL). All experiments were performed in triplicate and repeated at least three times.

Statistical analyses

Values are expressed as mean ± SD of at least three independent experiments and analyzed using one-way

ANOVA followed by Duncan's Multiple Range Test for comparisons of group means. All statistical analyses were performed using SPSS 18 for Windows, and P values < 0.05 were deemed to indicate statistical significance.

Results

FGF21 protects mice against D-gal-induced hepatic dysfunction

The extent of hepatic injury can be evaluated by measuring the serum activities or levels of ALT, AST, ALP, TBIL, and DBIL [24]. To determine whether FGF21 can attenuate the liver damage in the D-gal mice, we measured the activities of these parameters of all groups (Fig. 1). Comparing with the normal controls, the activities or levels of serum AST, ALP, TBIL, and DBIL increased significantly in untreated D-gal mice ($P < 0.01$). After 8 weeks treatment by FGF21, these parameters except ALT were suppressed in FGF21-treated groups ($P < 0.01$ or $P < 0.05$).

FGF21 treatment reduces D-gal-induced histological damage of the liver in mice

The liver histology was used to determine the protective effect of FGF21 on D-gal-induced injury. As shown in Fig. 2, compared with normal controls, D-gal treatment caused visible histological changes including structure damage, degeneration, and necrosis of hepatocytes (Fig. 2a, b). While high dose FGF21 (5 mg kg^{-1} d^{-1}) significantly alleviated the liver damage in D-gal-treated mice (Fig. 2c), low dose FGF21 (1 mg kg^{-1} d^{-1}) group showed midrange degeneration of hepatocytes (Fig. 2d).

FGF21 inhibits D-gal-induced oxidative stress by changing multiple oxidative stress parameters in mice

Many studies have suggested that the levels of ROS might be indicators of oxidative stress and stimulating ROS production is reported as one of the most important mechanisms underlying the D-gal-induced liver dysfunction. Our results (Fig. 3a) showed that D-gal-treatment caused a significant increase of ROS in the liver compared with normal control group ($P < 0.01$). After FGF21 administration for 2 months, the ROS levels in the liver tissue significantly reduced in a dose-dependent manner compared with untreated D-gal mice ($P < 0.01$ or $P < 0.05$).

We also detected most recognized oxidative damage product, MDA, which is a by-product of lipid peroxidation induced by free radicals. Our results (Fig. 3b) showed that D-gal treatment could induce an increase of the MDA level in the liver compared with normal controls ($P < 0.01$). This increase was reduced ($P < 0.05$) by FGF21 treatment (5 mg kg^{-1} d^{-1} or 1 mg kg^{-1} d^{-1}).

Next, we detected several key antioxidants which can scavenge ROS, including enzymatic antioxidants SOD, CAT, and GSH-Px, and non-enzymatic antioxidant T-AOC in the liver of D-gal-induced mice (Fig. 3c–f). In our results, a significant decrease in the activities of these antioxidants was observed in D-gal-treated mice compared with normal control group ($P < 0.001$ or $P < 0.01$). Administration of FGF21 significantly prevented the D-gal-induced decrease of enzymatic or non-enzymatic antioxidant activity in the liver ($P < 0.01$ or $P < 0.05$).

FGF21 attenuates ROS accumulation through increasing nuclear translocation of Nrf2 and the expression of antioxidant genes in the liver of D-gal-treated mice

Nrf2 is a transcription factor that regulates the expression of numerous ROS detoxifying and antioxidant genes. In order to test whether FGF21 could activate Nrf2, we detected the protein accumulations of Nrf2 in the nucleus. As shown in Fig. 4a, D-gal treatment significantly inhibited the protein accumulations of Nrf2 in the liver, and administration of FGF21 increased the accumulation of Nrf2 in nucleus ($P < 0.01$ or $P < 0.05$), suggesting that FGF21 treatment restores the antioxidant activities in the liver of D-gal mice by increasing the activity of Nrf2 transcriptional regulator.

As GSH has been demonstrated to be regulated by Nrf2 [9], we detected the levels of GSH in the liver of all groups. Comparing with normal controls, the GSH levels in the liver of D-gal mice were lower ($P < 0.01$) (Fig. 4b). Administration of FGF21 significantly reversed the decreased levels of GSH in the liver of D-gal mice in a dose-dependent manner ($P < 0.01$ or $P < 0.05$). Furthermore, FGF21 also significantly increased mRNA expression of several antioxidant genes of Nrf2 targets, such as Sod2, Gpx-1, G6pdh, and GCL-c in the liver of D-gal mice ($P < 0.01$ or $P < 0.05$) (Fig. 4c–f), suggesting that FGF21 administration may exert its protective effect on D-gal-induced oxidative stress in the liver by elevating multiple antioxidants genes.

FGF21 prevents D-gal-induced apoptosis of hepatocytes

We used the TUNEL assay to investigate the protective effect of FGF21 on D-gal-induced apoptosis (Fig. 5). The results showed that the number of TUNEL-positive cells in the liver of D-gal mice significantly increased comparing with normal controls ($P < 0.01$), whereas administration of FGF21 markedly decreased TUNEL-positive cells in the

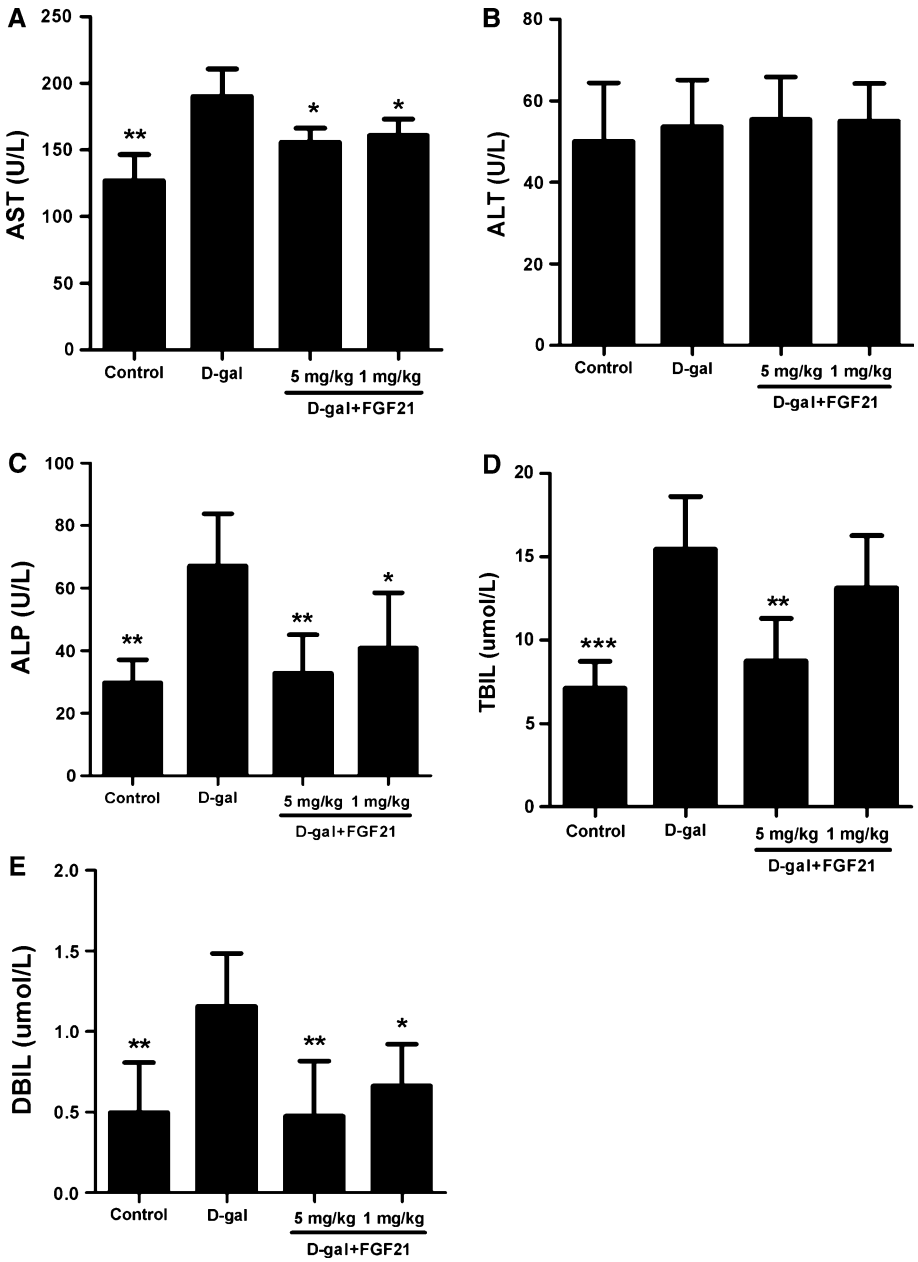

Fig. 1 Effect of FGF21 on D-gal-induced changes in hepatic functional markers. Normal controls were treated with saline (0.9 %), and D-gal mice were treated with D-gal daily for 8 weeks. FGF21-treated D-gal mice (D-gal + FGF21) were treated with D-gal and simultaneously administrated with FGF21 sc at doses of 1 or 5 mg kg^{-1} d^{-1} once a day for 8 weeks. **a** AST activity; **b** ALT activity; **c** ALP activity; **d** TBIL levels; **e** DBIL levels. All these parameters were measured by commercial detection kit. All data are represented as mean ± SD, $n = 8$ per group. *$P < 0.05$, **$P < 0.01$ and ***$P < 0.001$ versus D-gal group

liver of the D-gal mice ($P < 0.01$). In addition, No significant difference in the number of TUNEL-positive cells in the liver could be seen between the FGF21-treated mice (5 mg kg^{-1} d^{-1}) and normal controls.

FGF21 modulates PI3K-Akt activation and the expression of caspase-3 and pro-apoptotic proteins

PI3K/Akt pathway is one of the major intracellular signaling pathways for suppressing apoptosis and promoting cell survival [26]. To investigate whether PI3K-Akt signaling is involved in the action of FGF21, we determined the effects of FGF21 on PI3K/Akt pathway in the mouse liver. Western blotting (Fig. 6a–d) revealed that the levels of PI3K and phospho-Akt (Ser473) markedly decreased in the livers of D-gal mice as compared with the normal controls ($P < 0.01$). However, the down-regulation of PI3K and phospho-Akt (Ser473) was markedly reversed by treatment with FGF21 ($P < 0.01$ or $P < 0.05$). There were no significant changes of total Akt levels among all groups.

PI3K/Akt has been shown to regulate the expression of pro-apoptotic and anti-apoptotic members of the Bcl-2 family such as Bcl-2 and Bax, suggesting the involvement of the mitochondrial intrinsic pathway of apoptosis [27]. Therefore, we examined the effects of FGF21 on Akt-

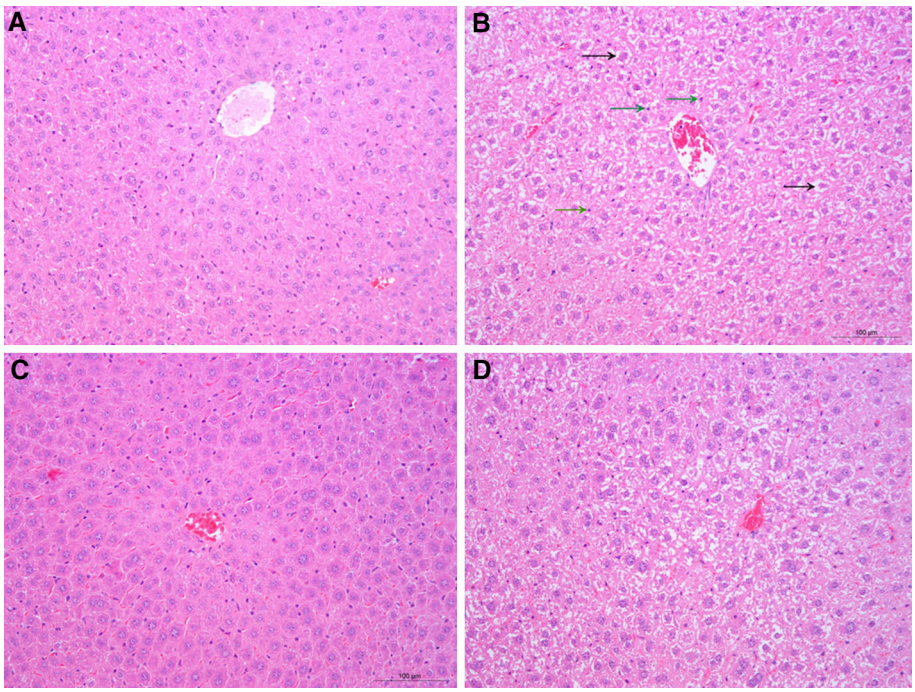

Fig. 2 Effect of FGF21 on histopathological changes of the D-gal-treated mouse liver. Normal controls were treated with saline (0.9 %), and D-gal mice were treated with D-gal daily for 8 weeks. FGF21-treated D-gal mice (D-gal + FGF21) were treated with D-gal and simultaneously administrated with FGF21 sc at doses of 1 or 5 mg kg^{-1} d^{-1} once a day for 8 weeks. **a** Normal control; **b** Mouse treated with D-gal at dose of 180 mg kg^{-1} d^{-1}; **c** FGF21-treated D-gal mice (D-gal + FGF21) (5 mg kg^{-1} d^{-1}). **d** FGF21-treated D-gal mice (D-gal + FGF21) (1 mg kg^{-1} d^{-1}). The *black arrow* indicates hepatic cell necrosis. The *green arrow* indicates the leukocytes. Original magnification, 10 × 20. (Color figure online)

regulated intrinsic pro-apoptotic proteins. As shown in Fig. 6e and h, D-gal caused a reduction in the expression of the anti-apoptotic protein Bcl-2 ($P < 0.01$) and increased the mitochondrial translocation of Bax in the mouse liver ($P < 0.01$). However, FGF21 treatment abolished the D-gal-evoked pro-apoptotic signaling events in the liver of mice ($P < 0.01$ or $P < 0.05$).

Caspase-3 is one of the key executioners of apoptosis, capable of cleaving or degrading many key proteins such as nuclear lamins, fodrin, and the nuclear enzyme poly (ADPribose) polymerase (PARP) [28]. To determine the effects of FGF21 on caspase-3 activation, we detected endogenous levels of the large fragment (17/19 kDa) of activated caspase-3 in the mouse liver (Fig. 6i, j). Comparing with the normal controls, the levels of activated caspase-3 were significantly elevated in the liver of D-gal mice ($P < 0.01$). Treatment with FGF21 inhibited this elevation in a dose-dependent manner ($P < 0.01$ or $P < 0.05$).

The p21 protein is thought to be a major effector of p53 activity in senescent cells, which induces apoptosis or telomere loss [29]. In the mice livers, p53/p21 activation primarily results in cell cycle arrest [30]. As shown in Fig. 6k, our results showed that the mRNA expression of P21 significantly increased in the liver of D-gal mice ($P < 0.01$). Administration of FGF21 (5 mg kg^{-1} d^{-1}) attenuated the increase of P21 in the liver of D-gal mice ($P < 0.05$).

Discussion

The liver is a major organ involved in D-gal metabolism and D-gal treatment is found to increase hepatic MDA levels and cause DNA damage together with oxidative stress [31]. Age-related disease model, such as liver injury, induced by D-gal treatment (100–500 mg/kg body weight; s.c.) for 8 weeks to rats or mice has been widely accepted [24, 25, 31]. The chronic subcutaneous administration of D-gal for 7 weeks induces oxidative stress and hepatopathy in mice and significantly decreases the hepatic superoxide dismutase and glutathione peroxidase activities [32]. However, there is no report about the FGF21 protective effects on liver injury induced by D-gal.

Previous studies have shown that treatment with D-gal causes liver injury and dysfunction, followed by elevated activities or levels of serum enzymes and histopathological damage [24, 25, 31, 32]. Our results also showed that the activities or the levels of AST, ALP, TBIL, and DBIL in the serum of D-gal mice were markedly increased.

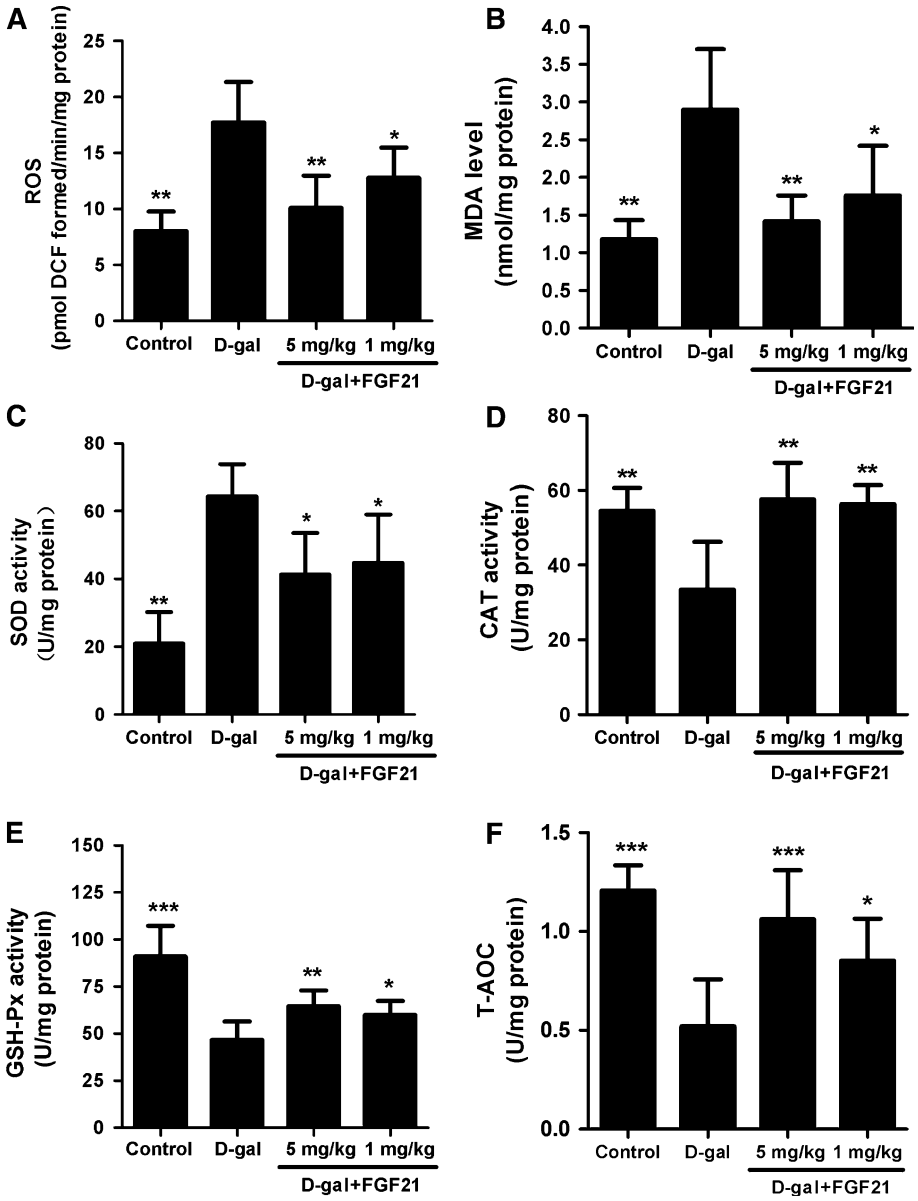

Fig. 3 Effect of FGF21 on the production of ROS and the parameters of oxidative stress in the liver of D-gal-treated mice. Normal controls were treated with saline (0.9 %), and D-gal mice were treated with D-gal daily for 8 weeks. FGF21-treated D-gal mice (D-gal + FGF21) were treated with D-gal and simultaneously administrated with FGF21 sc at doses of 1 or 5 mg kg^{-1} d^{-1} once a day for 8 weeks. **a** ROS were measured with 2, 7-dichlorofluorescein-diacetate (DCFH-DA) fluorescence and determined using Fluorescence Microplate Reader (Perkin Elmer, America). **b**, **c** MDA level and SOD activity were measured by commercial detection kit using Microplate Reader (Biotech Elx800). **d**–**f** CAT, GSH-Px, and T-AOC activities were measured by commercial detection kit using 722 spectrophotometer. All data are represented as mean ± SD, $n = 8$ per group. $^{*}P < 0.05$, $^{**}P < 0.01$ and $^{***}P < 0.001$ versus D-gal group

Moreover, histological changes of the liver, such as structure damage, degeneration, and necrosis, had been observed. In this study, treatment with FGF21 effectively protected mice against D-gal-induced liver damage as indicated that the activities or the levels of serum AST, ALP, TBIL, and DBIL decreased and hepatic histological changes were alleviated, suggesting a protective effect of FGF21 against D-gal-induced liver injury.

Many studies demonstrate that possible molecular mechanism involved in D-gal-induced hepatotoxicity is the disruption of delicate oxidant/antioxidant balance, which can lead to liver injury via oxidative damage. Accumulating evidence has also shown that ROS generation induced by D-gal is a major reason resulting in oxidative stress [25, 31]. In the present study, we showed that D-gal induced overproduction of ROS in the mice and led to hepatic oxidative damage, and the level of oxidative marker MDA, which indicates the degree of lipid peroxidation, significantly increased compared with normal controls. FGF21 has been proven to prevent oxidative stress and posses potent antioxidant/free radical-scavenging properties [16, 18, 33]. Our results showed that FGF21 decreased the ROS production and MDA level in the liver of D-gal mice, suggesting that FGF21 protects the liver against oxidative stress induced by D-gal by decreasing ROS and the lipid peroxide level. It is well known that the defense system of antioxidant enzymes containing SOD, CAT, GSH-Px, and so on may reduce oxidative stress and potentially benefit oxidative-related diseases [34]. Oxidative stress could enhance generation of free radical and impair

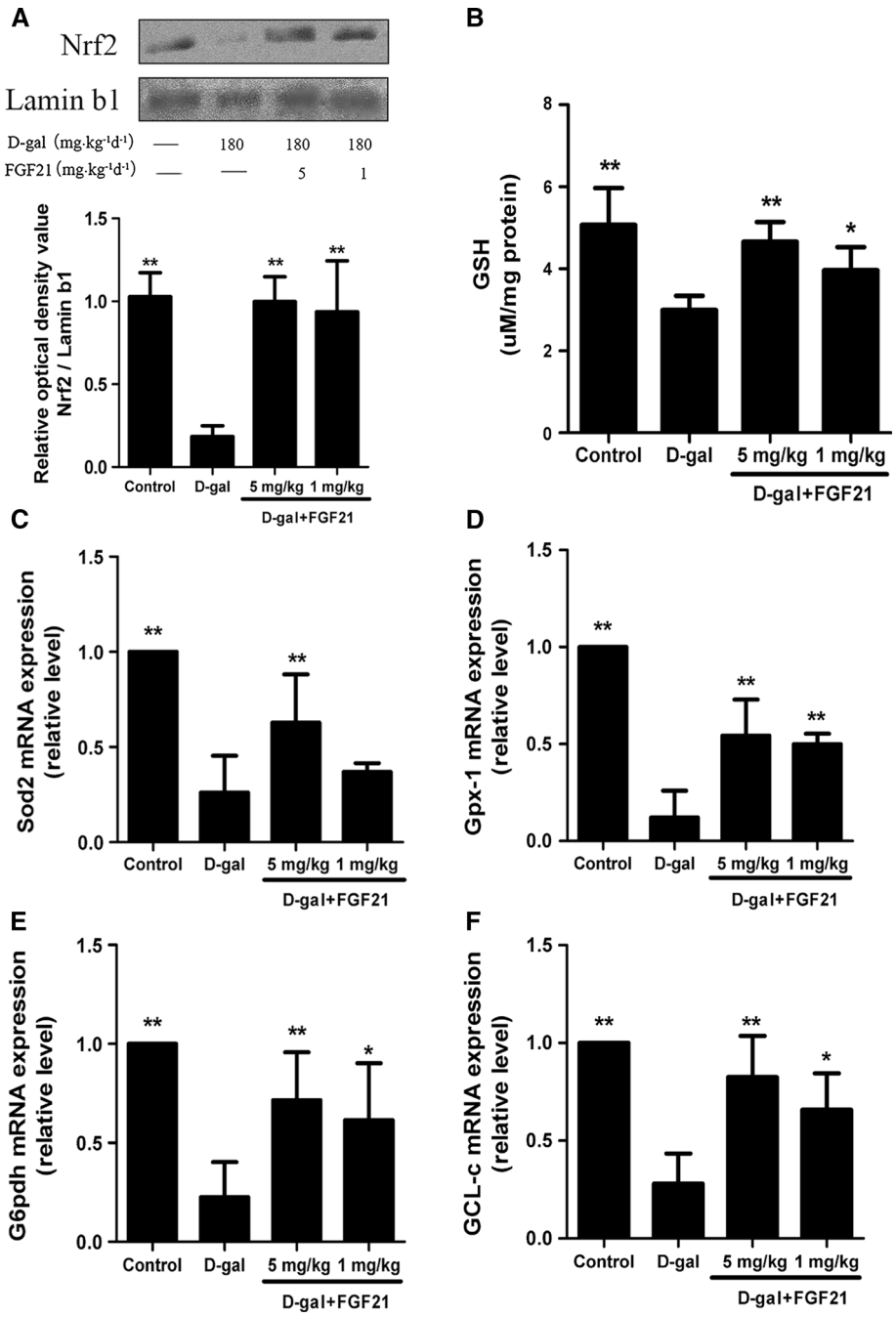

Fig. 4 FGF21 induces nuclear abundance of Nrf2 and increases the levels of GSH and the expression of antioxidant genes in the liver of D-gal mice. Normal controls were treated with saline (0.9 %), and D-gal mice were treated with D-gal daily for 8 weeks. FGF21-treated D-gal mice (D-gal + FGF21) were treated with D-gal and simultaneously administrated with FGF21 sc at doses of 1 or 5 mg kg^{-1} d^{-1} once a day for 8 weeks. **a** The protein levels of Nrf2 in the nucleus were determined by Western blot analysis. The relative density is expressed as the ratio Nrf2/Laminb1. The bands were analyzed with Image pro plus and the normal control is set as 1.0. **b** Hepatic levels of GSH were determined by commercial detection kit using Microplate Reader (Biotech Elx800). **c** mRNA expression of Sod2. **d** mRNA expression of Gpx-1. **e** mRNA expression of G6pdh. **f** mRNA expression of GCL-c. The mRNA expression was quantified by real-time PCR. Expression of each gene relative to the expression of housekeeping gene, β-actin was analyzed and calculated as $2^{-\Delta\Delta Ct}$. All data are represented as mean ± SD, $n = 8$ per group. $^{*}P < 0.05$, $^{**}P < 0.01$ and $^{***}P < 0.001$ versus D-gal group

enzymatic antioxidant or non-enzymatic antioxidant. The present study showed that the activities of antioxidant enzymes, including SOD, CAT, GSH-Px, and T-AOC, were dramatically decreased in the liver of D-gal mice. Interestingly, FGF21 could markedly renew the activities of those antioxidants enzymes in the livers of D-gal mice.

The transcription factor Nrf2, which normally exists in an inactive state as a consequence of binding to a cytoskeleton-associated protein, Keap1, can be activated by redox-dependent stimuli. Alteration of the Nrf2-Keap1 interaction enables Nrf2 to translocate to the nucleus, bind to the antioxidant-responsive element (ARE), and initiate the transcription of genes coding for detoxifying enzymes and cytoprotective proteins [35]. It has been reported that Nrf2 is an important factor in controlling both constitutive and inducible expression of a wide spectrum of antioxidants and is responsible for protecting cells against oxidative stress induced by D-gal in mice [36]. Our present study showed that D-gal-induced decreased Nrf2 translocation and its targeted antioxidant genes expression, such

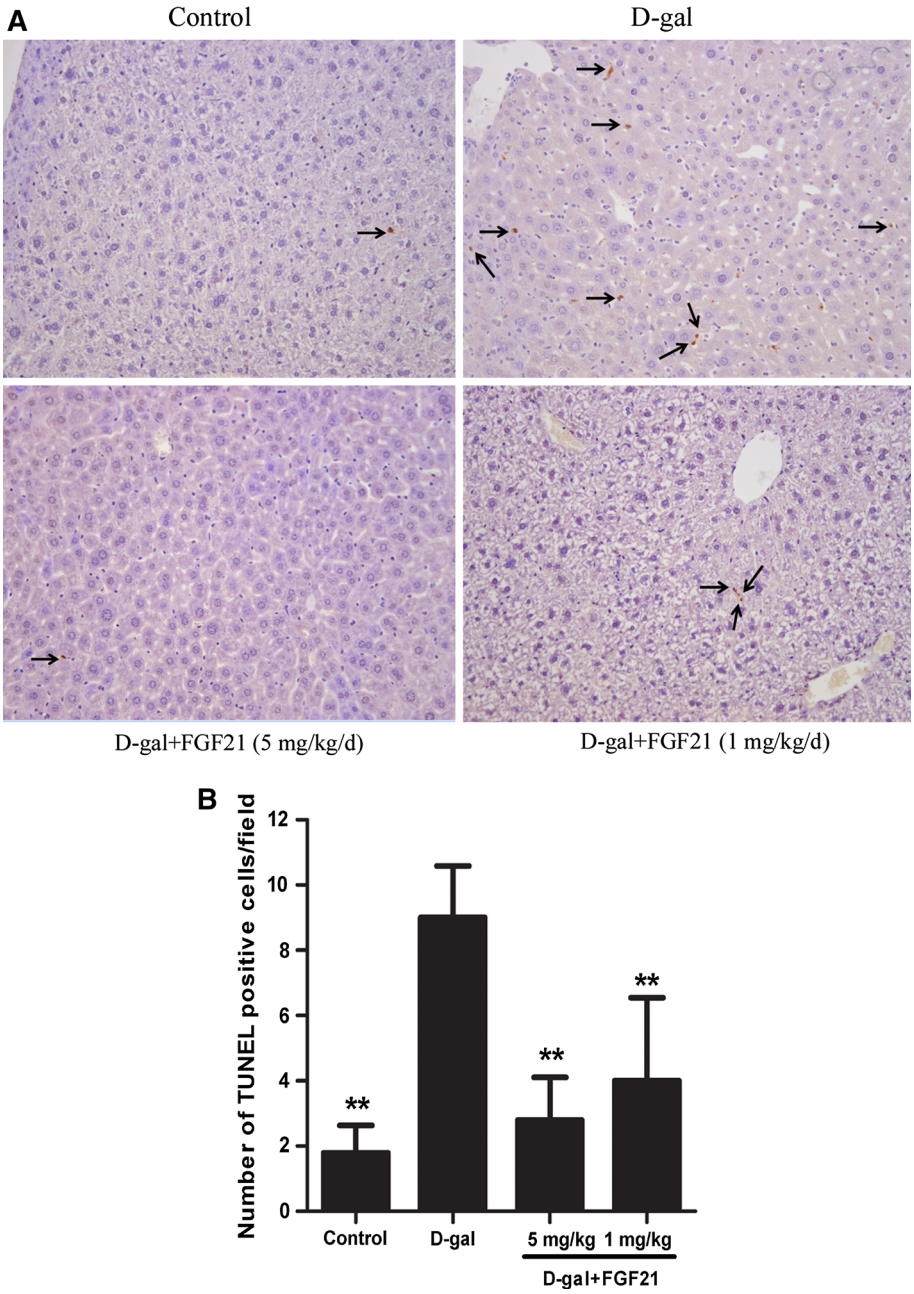

Fig. 5 FGF21 prevents D-gal-induced apoptosis of hepatocytes. Normal controls were treated with saline (0.9 %), and D-gal mice were treated with D-gal daily for 8 weeks. FGF21-treated D-gal mice (D-gal + FGF21) were treated with D-gal and simultaneously administrated with FGF21 sc at doses of 1 or 5 mg kg^{-1} d^{-1} once a day for 8 weeks. Liver apoptosis was examined with TUNEL staining. **a** Representative micrographs of hepatic TUNEL staining from mice in all groups, Magnification, 10 × 20. **b** Quantitative results of hepatic TUNEL staining. All data are represented as mean ± SD, $n = 8$ per group. $^{*}P < 0.05$, $^{**}P < 0.01$ and $^{***}P < 0.001$ versus D-gal group

as Sod2, Gpx-1, G6pdh, and GCL-c in the liver of mice. Whereas administration of FGF21 is sufficient to reverse these changes, suggesting that FGF21 protects mouse liver against D-gal-induced oxidative stress by regulating the activation of Nrf2 and Nrf2-mediated expression of antioxidant genes. Recently, it has been demonstrated that FGF21 is able to protect against Acetaminophen-induced hepatotoxicity by enhancing PGC-1α/Nrf2-mediated antioxidant capacity in the liver [22]. GSH, which has been demonstrated to be regulated by Nrf2, is an important intracellular antioxidant and redox potential regulator that plays a vital role in drug detoxification and elimination and in cellular protection from damage by ROS, peroxides, and toxins [9, 37]. It is also reported that the initiation of apoptosis is associated with the depletion of intracellular GSH and the elevation of GSH level can protect cell from apoptosis [38]. In the present study, the results showed that GSH level decreased significantly in the liver of D-gal mice comparing with normal controls, and administration of FGF21 significantly increased hepatic GSH levels in a dose-dependent manner.

PI3K/Akt signaling is known to protect a variety of cells from apoptosis [25]. Akt, which is the primary mediator of PI3K-initiated signaling, can be phosphorylated and

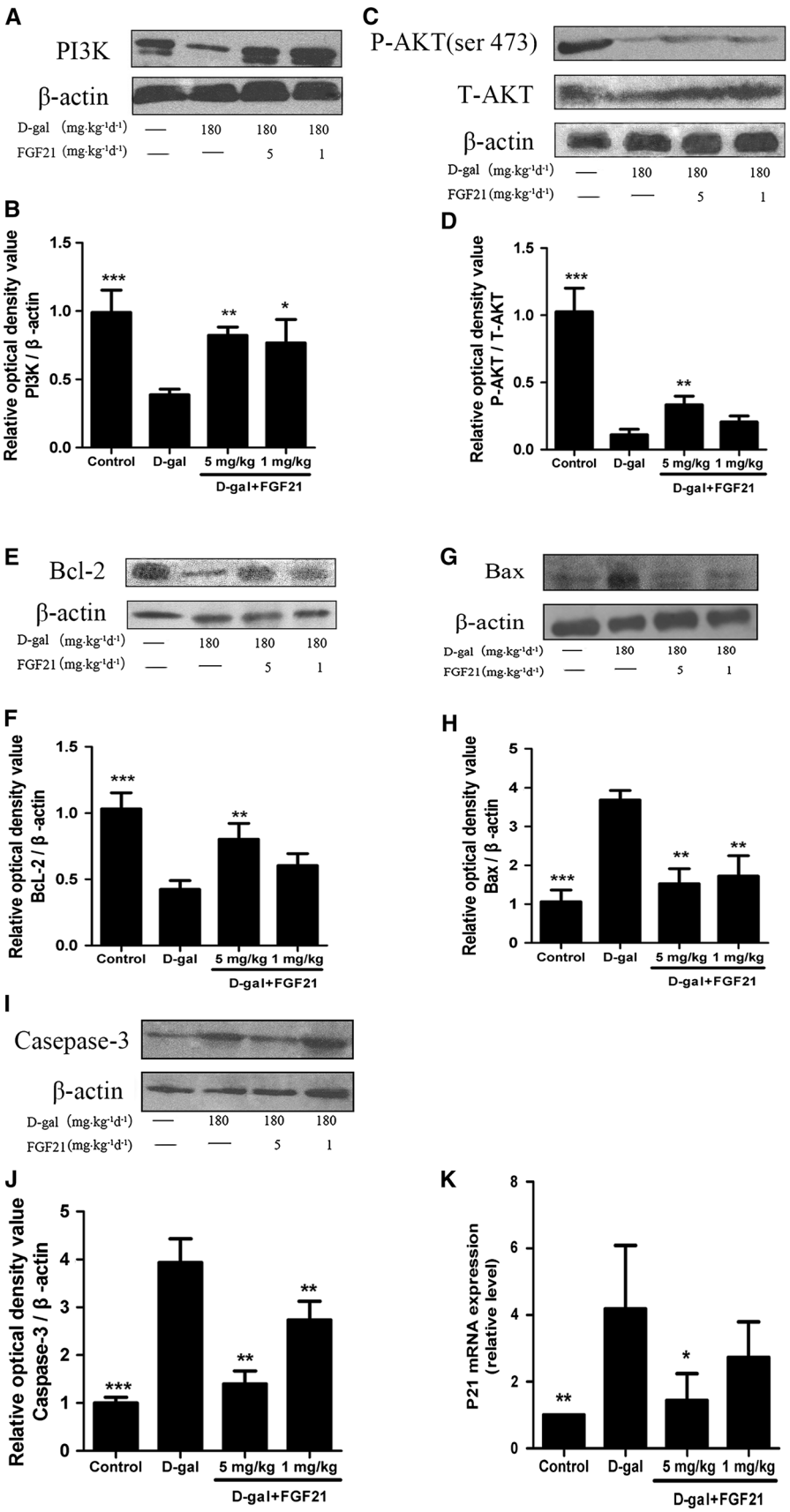

Fig. 6 FGF21 regulates the PI3K-Akt pathway and the expression of caspase-3 and pro-apoptotic proteins in the liver of D-gal mice. Normal controls were treated with saline (0.9 %), and D-gal mice were treated with D-gal daily for 8 weeks. FGF21-treated D-gal mice (D-gal + FGF21) were treated with D-gal and simultaneously administrated with FGF21 sc at doses of 1 or 5 mg kg^{-1} d^{-1} once a day for 8 weeks. **a**, **c**, **e**, **g**, **i** Western blots for PI3K, phospho-Akt (Ser473), Bcl-2, Bax, and caspase-3 of the liver in mice. **b**, **d**, **f**, **h**, **j** Fold change in relative density analysis of PI3K, phospho-Akt (Ser473), Bcl-2, Bax, and caspase-3 protein bands. β-actin was probed as an internal control in relative density analysis of the protein bands. The relative density is expressed as the ratio (PI3K/β-actin, phospho-Akt/Total-Akt, Bcl-2/β-actin, Bax/β-actin, Bax/β-actin, and caspase-3/β-actin). The bands were analyzed with Image pro plus and the vehicle control is set as 1.0. Values are averages from three independent experiments. **k** mRNA expression of P21. All data are represented as mean ± SD, $n = 8$ per group. $^{*}P < 0.05$, $^{**}P < 0.01$ and $^{***}P < 0.001$ versus D-gal group

activated at residues Ser473. It has been well established that Akt acts as an anti-apoptotic signaling molecule in many different cell death paradigms [39]. It has also been reported that the PI3K/Akt pathway is involved in Nrf2-dependent transcription [40]. In this study, we found that the expression levels of PI3K p110 and Akt phosphorylation decreased in the liver of D-gal-treated mice. Administration of FGF21 significantly increased hepatic levels of PI3K p110 and Akt phosphorylation in D-gal-treated mice, suggesting that FGF21 could protect mouse liver by regulating the PI3K-Akt signaling pathway.

PI3K/Akt signaling can up-regulate the expression of Bcl-2, and activated Akt can also regulate cellular survival and metabolism by binding and regulating many downstream effectors, such as Bcl-2 family proteins [41]. Bcl-2 family proteins, including Bcl-2 and Bax, play important anti-apoptotic roles in the mitochondrial apoptotic pathway and it can inhibit the release of cytochrome c from mitochondria into the cytosol. Once released, cytochrome c and apoptotic peptidase activating factor 1 (Apaf-1) coassemble in the presence of dATP to form the apoptosome which induces caspase 9 dimerization and autocatalysis. Activated caspase 9 stimulates caspase 3 and subsequent cell apoptosis [41]. In this study, our results showed that FGF21 significantly reduced the expression of Bax and increased the expression of the anti-apoptotic protein Bcl-2 in the liver of D-gal mice. Caspase is a family of proteins that are main executors of the apoptotic process, which is a well-identified downstream target for PI3K-Akt [12, 28]. Caspase-3 plays a central role in the execution-phase of cell apoptosis. Once activated, caspase-3 can in turn cleave other protein substrates within the cell, and result in the apoptotic process [42]. The present study showed that FGF21 decreased the number of TUNEL-positive cells and levels of activated caspase-3 in the livers of D-gal-treated mice. ROS could activate caspase-3, thereby resulting in apoptosis [42]. So our findings suggested that the inhibition of caspase-3 activation might attribute to powerful ROS scavenging and antioxidant activities of FGF21.

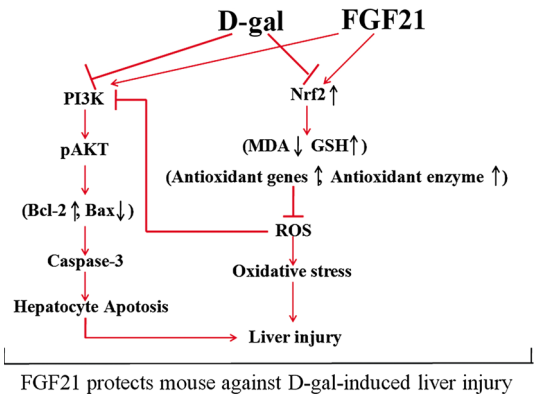

Fig. 7 Schematic diagram shows the signaling of FGF21 on D-gal-induced liver damage. *Rightwards arrow* indicates activation or induction, and *rightwards line from bar* indicates inhibition or blockade

Conclusion

In summary, this study demonstrates for the first time that FGF21 has potent protective effects against D-gal-induced oxidative stress via activating Nrf2, which in turn triggers PI3K/Akt-mediated apoptosis pathways in the mouse liver. Hypothetic signaling pathway for FGF21 protecting against D-gal-induced liver injury is illustrated in Fig. 7. This study provides a novel insight into the mechanisms of FGF21 in the protection of the liver.

Acknowledgments Yinhang Yu, Fuliang Bai, Wenfei Wang, and Deshan Li conceived and designed the experiments. Yinhang Yu, Yaonan Liu, Yongbi Yang, Qingyan Yuan, Dehua Zou, Tong Zhang, Siming Li, Susu Qu, Guiyou Tian, and YunYe Liu performed the experiments. Yin hang Yu, Guiping Ren, and Deshan Li analyzed the data. Yinhang Yu wrote the paper. Deshan Li revised the paper.

Conflict of interest The authors declare no conflicts of interest.

References

1. Cui X, Wang L, Zuo P, Han Z, Fang Z, Li W, Liu J (2004) D-Galactose-caused life shortening in *Drosophila melanogaster* and *Musca domestica* is associated with oxidative stress. Biogerontology 5:317–325
2. Lu J, Zheng YL, Wu DM, Luo L, Sun DX, Shan Q (2007) Ursolic acid ameliorates cognition deficits and attenuates oxidative damage in the brain of senescent mice induced by D-galactose. Biochem Pharmacol 74:1078–1090
3. Ho SC, Liu JH, Wu RY (2003) Establishment of the mimetic aging effect in mice caused by D-galactose. Biogerontology 4:15–18
4. Ramana BV, Kumar VV, Krishna PN, Kumar CS, Reddy PU, Raju TN (2006) Effect of quercetin on galactose-induced hyperglycaemic oxidative stress in hepatic and neuronal tissues of Wistar rats. Acta Diabetol 43:135–141
5. Long JG, Wang XM, Gao HX, Liu Z, Liu CS, Miao MY, Cui X, Packer L, Liu JK (2007) D-Galactose toxicity in mice is associated with mitochondrial dysfunction: protecting effects of mitochondrial nutrient R-alpha-lipoic acid. Biogerontology 8:373–381
6. Chandra J, Samali A, Orrenius S (2000) Triggering and modulation of apoptosis by oxidative stress. Free Radic Biol Med 29:323–333
7. Simon HU, Haj-Yehia A, Levi-Schaffer F (2000) Role of reactive oxygen species (ROS) in apoptosis induction. Apoptosis 5:415–418
8. Jacob MH, Janner Dda R, Araújo AS, Jahn MP, Kucharski LC, Moraes TB, Dutra Filho CS, Ribeiro MF, Belló-Klein A (2010) Redox imbalance influence in the myocardial Akt activation in aged rats treated with DHEA. Exp Gerontol 45:957–963
9. Harvey CJ, Thimmulappa RK, Singh A, Blake DJ, Ling G, Wakabayashi N, Fujii J, Myers A, Biswal S (2009) Nrf2-

regulated glutathione recycling independent of biosynthesis is critical for cell survival during oxidative stress. Free Radic Biol Med 46:443–453
10. Cho SG, Choi EJ (2002) Apoptotic signaling pathways: caspases and stress-activated protein kinases. J Biochem Mol Biol 35:24–27
11. Porta C, Figlin RA (2009) Phosphatidylinositol-3-kinase/Akt signaling pathway and kidney cancer, and the therapeutic potential of phosphatidylinositol-3-kinase/Akt inhibitors. J Urol 182:2569–2577
12. Liu CM, Ma JQ, Sun YZ (2012) Puerarin protects rat kidney from lead-induced apoptosis by modulating the PI3K/Akt/eNOS pathway. Toxicol Appl Pharmacol 258:330–342
13. Kharitonenkov A, Shiyanova TL, Koester A, Ford AM, Micanovic R, Galbreath EJ, Sandusky GE, Hammond LJ, Moyers JS, Owens RA, Gromada J, Brozinick JT, Hawkins ED, Wroblewski VJ, Li DS, Mehrbod F, Jaskunas SR, Shanafelt AB (2005) FGF-21 as a novel metabolic regulator. J Clin Invest 115:1627–1635
14. Ryden M (2009) Fibroblast growth factor 21: an overview from a clinical perspective. Cell Mol Life Sci 66:2067–2073
15. Wente W, Efanov AM, Brenner M, Kharitonenkov A, Köster A, Sandusky GE, Sewing S, Treinies I, Zitzer H, Gromada J (2006) Fibroblast growth factor-21 improves pancreatic beta-cell function and survival by activation of extracellular signal-regulated kinase 1/2 and Akt signaling pathways. Diabetes 55:2470–2478
16. Feingold KR, Grunfeld C, Heuer JG, Gupta A, Cramer M, Zhang T, Shigenaga JK, Patzek SM, Chan ZW, Moser A, Bina H, Kharitonenkov A (2012) FGF21 is increased by inflammatory stimuli and protects leptin-deficient ob/ob mice from the toxicity of sepsis. Endocrinology 153:2689–2700
17. Planavila A, Redondo I, Hondares E, Vinciguerra M, Munts C, Iglesias R, Gabrielli LA, Sitges M, Giralt M, van Bilsen M, Villarroya F (2013) Fibroblast growth factor 21 protects against cardiac hypertrophy in mice. Nat Commun 4:2019
18. Cong WT, Ling J, Tian HS, Ling R, Wang Y, Huang BB, Zhao T, Duan YM, Jin LT, Li XK (2013) Proteomic study on the protective mechanism of fibroblast growth factor 21 to ischemia–reperfusion injury. Can J Physiol Pharmacol 91:973–984
19. Potthoff MJ, Inagaki T, Satapati S, Ding X, He T, Goetz R, Mohammadi M, Finck BN, Mangelsdorf DJ, Kliewer SA, Burgess SC (2009) FGF21 induces PGC-1alpha and regulates carbohydrate and fatty acid metabolism during the adaptive starvation response. Proc Natl Acad Sci USA 106:10853–10858
20. Inagaki T, Dutchak P, Zhao G, Ding X, Gautron L, Parameswara V, Li Y, Goetz R, Mohammadi M, Esser V, Elmquist JK, Gerard RD, Burgess SC, Hammer RE, Mangelsdorf DJ, Kliewer SA (2007) Endocrine regulation of the fasting response by PPARalpha-mediated induction of fibroblast growth factor 21. Cell Metab 5:415–425
21. Inagaki T, Lin VY, Goetz R, Mohammadi M, Mangelsdorf DJ, Kliewer SA (2008) Inhibition of growth hormone signaling by the fasting-induced hormone FGF21. Cell Metab 8:77–83
22. Ye D, Wang Y, Li H, Jia W, Man K, Lo CM, Wang Y, Lam KS, Xu A (2014) FGF21 Protects against acetaminophen-induced hepatotoxicity by potentiating PGC-1α-mediated antioxidant capacity in mice. Hepatology. doi:10.1002/hep.27060
23. Guicciardi ME, Gores GJ (2005) Apoptosis: a mechanism of acute and chronic liver injury. Gut 54:1024–1033
24. Ruan Q, Liu F, Gao Z, Kong D, Hu X, Shi D, Bao Z, Yu Z (2013) The anti-inflamm-aging and hepato protective effects of huperzine A in D-galactose-treated rats. Mech Ageing Dev 134:89–97
25. Zhang ZF, Lu J, Zheng YL, Hu B, Fan SH, Wu DM, Zheng ZH, Shan Q, Liu CM (2010) Purple sweet potato color protects mouse liver against D-galactose-induced apoptosis via inhibiting caspase-3 activation and enhancing PI3K/Akt pathway. Food Chem Toxicol 48:2500–2507
26. Rana SV (2008) Metals and apoptosis: recent developments. J Trace Elem Med Biol 22:262–284
27. Franco R, Sánchez-Olea R, Reyes-Reyes EM, Panayiotidis MI (2009) Environmental toxicity, oxidative stress and apoptosis: ménage à trois. Mutat Res 674:3–22
28. Lawen A (2003) Apoptosis—an introduction. BioEssays 25:888–896
29. Itahana K, Zou Y, Itahana Y, Martinez JL, Beausejour C, Jacobs JJ, Van Lohuizen M, Band V, Campisi J, Dimri GP (2003) Control of the replicative life span of human fibroblasts by p16 and the polycomb protein Bmi-1. Mol Cell Biol 2:389–401
30. Satyanarayana A, Wiemann SU, Buer J, Lauber J, Dittmar KE, Wustefeld T, Blasco MA, Manns MP, Rudolph KL (2003) Telomere shortening impairs organ regeneration by inhibiting cell cycle re-entry of a subpopulation of cells. EMBO J 22:4003–4013
31. Zhang ZF, Fan SH, Zheng YL, Lu J, Wu DM, Shan Q, Hu B (2009) Purple sweet potato color attenuates oxidative stress and inflammatory response induced by D-galactose in mouse liver. Food Chem Toxicol 47:496–501
32. Chen HL, Wang CH, Kuo YW, Tsai CH (2011) Antioxidative and hepatoprotective effects of fructo-oligosaccharide in D-galactose-treated Balb/cJ mice. Br J Nutr 105:805–809
33. Zhang C, Shao M, Yang H, Chen L, Yu L, Cong W, Tian H, Zhang F, Cheng P, Jin L, Tan Y, Li X, Cai L, Lu X (2013) Attenuation of hyperlipidemia- and diabetes-induced early-stage apoptosis and late-stage renal dysfunction via administration of fibroblast growth factor-21 is associated with suppression of renal inflammation. PLoS One 8:e82275
34. Sun Y (1990) Free radicals, antioxidant enzymes, and carcinogenesis. Free Radic Biol Med 8:583–599
35. Kaspar JW, Niture SK, Jaiswal AK (2009) Nrf 2:INrf2 (Keap1) signaling in oxidative stress. Free Radic Biol Med 47:1304–1309
36. Li YN, Guo Y, Xi MM, Yang P, Zhou XY, Yin S, Hai CX, Li JG, Qi XJ (2014) Saponins from *Aralia taibaiensis* attenuate D-galactose-induced aging in rats by activating FOXO3a and Nrf2 pathways. Oxid Med Cell Longev. doi:10.1155/2014/320513
37. Wu JH, Batist G (2013) Glutathione and glutathione analogues, therapeutic potentials. Biochim Biophys Acta 1830:3350–3353
38. Han YH, Kim SZ, Kim SH, Park WH (2008) Arsenic trioxide inhibits the growth of Calu-6 cells via inducing a G2 arrest of the cell cycle and apoptosis accompanied with the depletion of GSH. Cancer Lett 18:40–55
39. Franke TF, Hornik CP, Segev L, Shostak GA, Sugimoto C (2003) PI3K/Akt and apoptosis: size matters. Oncogene 22:8983–8998
40. Yin F, Liu J, Zheng X, Guo L, Xiao H (2010) Geniposide induces the expression of heme oxygenase-1 via PI3K/Nrf2-signaling to enhance the antioxidant capacity in primary hippocampal neurons. Biol Pharm Bull 33:1841–1846
41. Pugazhenthi S, Nesterova A, Sable C, Heidenreich KA, Boxer LM, Heasley LE, Reusch JE (2000) Akt/protein kinase B up-regulates Bcl-2 expression through cAMP-response element-binding protein. J Biol Chem 275:10761–10766
42. Higuchi M, Honda T, Proske RJ, Yeh ET (1998) Regulation of reactive oxygen species-induced apoptosis and necrosis by caspase 3-like proteases. Oncogene 17:2753–2760